Depending upon the relationship between the quantities τ_{ind} and τ_m, one or the other equilibrium concentration of soot particles in the flame is reached. The induction time τ_{ind} is then basically determined by the thermokinetic characteristics of the process, while the mixing time τ_m is determined by the turbulence characteristics of the gas flow.

The second portion of this study will be dedicated to questions related to calculation of the induction time and the dynamics of carbon complex formation. A third part will consider the effect on the soot formation process of the turbulent flame microstructure.

LITERATURE CITED

1. A. G. Blokh, Heat Transport in Vapor Boiler Furnaces [in Russian], Leningrad (1984).
2. N. V. Lavrov, Physicochemical Fundamentals of the Fuel Combustion Process [in Russian], Moscow (1971).
3. N. Z. Magaril, The Mechanism and Kinetics of Homogeneous Thermal Hydrocarbon Conversions [in Russian], Moscow (1970).
4. N. M. Émmanuél' and D. G. Knorre, Course in Chemical Kinetics [in Russian], Moscow (1969).
5. A. I. Shelokov, Distribution and Combustion of Gas, Issue 3 [in Russian], Saratov (1977), pp. 141-150.

ROTATIONAL INSTABILITY OF THE LAMINAR FLOW OF PSEUDOPLASTIC FLUIDS IN A COAXIAL-CYLINDRICAL CHANNEL*

S. Vron'ski and M. Yastrzhembski

UDC 532.582.82

Measurements of the stability limit of a spiral flow of a non-Newtonian fluid ($n \leq 1$) in a coaxial-cylindrical channel are presented and substantiated.

INTRODUCTION

Many problems in mechanical and chemical engineering involve the motion of a fluid in an annular slit with a rotating cylindrical inside surface and a stagnant outside surface: the cooling of the rotors of electrical machinery [1]; dynamic filtration on a cylindrical interface [2]; the lubrication of bearings [3]; the operation of electrochemical reactors with a rotating cylindrical electrode [4]. Such flows are termed spiral flows and offer a particular advantage for high-viscosity pseudoplastic fluids. In this case, it is possible to reach high shear rates regardless of how long the fluid has been in the unit, i.e., regardless of the flow rate [5].

In the hydrodynamic analysis of spiral laminar flows, special attention is paid to the problem of their stability. Numerous theoretical and experimental studies have been conducted for Newtonian fluids. A survey of these investigations can be found in [6-8]. It is well known that a rotational flow becomes unstable when the angular velocity of the moving cylinder is sufficiently high. In this case, there is an abrupt disturbance of the axial (longitudinal) head flow. The boundaries of stability of the spiral flow are determined by two dimensionless parameters: the axial Reynolds number and the critical value of the rotational Taylor number. Within the region of small Re, the critical value of Ta increases monotonically with an increase in Re. The monotonic stabilization of circular Couette flow by the axial flow is disturbed at sufficiently high Re and the value of Ta_c decreases slightly with a further increase in Re [6]. The rotational instability of spiral flow is known to be

*Z. P. Shul'man, a member of the editorial staff of Inzhenerno-Fizicheskii Zhurnal, arranged for the publication of this article.

Institute of Chemical and Process Engineering of the Warsaw Polytechnic Institute.

Translated from Inzhenerno-Fizicheskii Zhurnal, Vol. 59, No. 3, pp. 499-508, September, 1990. Original article submitted September 18, 1989.

0022-0841/90/5903-1196$12.50

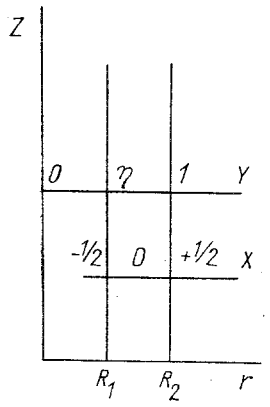

Fig. 1. Coordinate system.

connected with the generation of secondary flows: toroidal (axisymmetric) eddies at Re < 40 and spiral (nonaxisymmetric) eddies at Re > 40 [8].

Most theoretical studies of the stability of spiral flows have been based on the use of the method of small perturbations. Investigators have examined both of the above-mentioned types of secondary flows: 1) toroidal eddies [7]; 2) spiral eddies [8]. The linearized analysis for toroidal eddies agrees well with the experimental data at Re < 40. For large values of Re, the assumption of axisymmetric secondary flows leads to values of Ta_c which exceed the critical value established experimentally. The theoretical predictions based on the assumption that spiral eddies are present are in complete agreement with experimental findings [8].

The stability of the spiral flow of linearly viscoelastic fluids has been studied theoretically and experimentally within a limited range of parameters: it has been suggested that low shear elasticity has a destabilizing effect on rotational motion of the fluid. The stability of spiral flows of non-Newtonian fluids with variable viscosity has not yet been studied.

The problem of the stability of Couette flow (which can be regarded as the limiting case of spiral flow) has been studied for viscoelastic [10, 11] and purely viscous non-Newtonian fluids [12-14]. The complex hydrodynamics of the laminar spiral flow of non-Newtonian fluids creates methodological problems insofar as finding the stability limit is concerned. The apparent viscosity of the fluid changes over the entire annular slit, which makes it very difficult to select appropriate dimensionless parameters.

In the present investigation, we will examine the stability of the flow of pseudoplastic fluids at Re < 200. We will examine two of the most important questions related to this subject: the effect of pseudoplasticity on the onset of stability; the dependence of the stability limit on the size of the annular slit $\eta = (R_1/R_2)$. The experimental method is based on measurements of mass transfer from the surface of the internal cylinder. We use a power flow "law" to describe the mechanical behavior of the fluids.

1. Theoretical Premises. Laminar Flows of "Power-Law" Fluids

The velocity of a spiral flow has two nontrivial components. Their distribution is expressed by the following formulas [15] (cylindrical coordinates, Fig. 1):

$$V(y)/V_m = (1-\eta^2)\int_\eta^y (y' - k^2/y')\, f(y',\ B,\ k)\, \partial y' / \int_\eta^1 y^2(y^2 - k^2/y)\, f(y,\ B,\ k)\, dy, \tag{1}$$

$$\omega(y)/\omega_i = 1 - \int_\eta^y (1/y')^3 f(y',\ B,\ k)\, dy' / \int_\eta^1 (1/y^3)\, f(y,\ B,\ k)\, dy, \tag{2}$$

where

$$f(y,\ B,\ k) = (B^2(y - k^2/y)^2 + 1/y^4)^p. \tag{3}$$

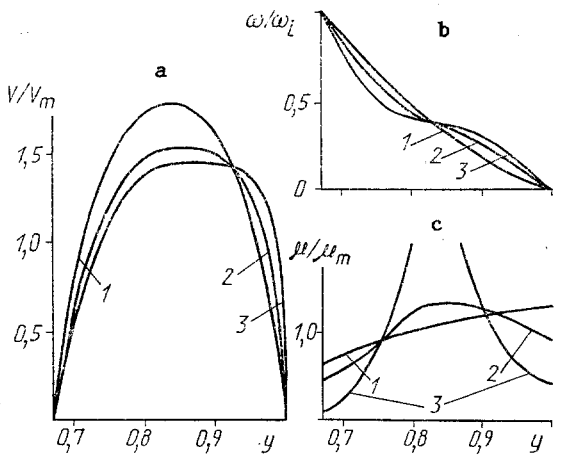

Fig. 2. Profiles of axial (a) and peripheral (b) velocity and viscosity (c) in a laminar spiral flow of a pseudoplastic fluid: n = 0.64, η = 0.66; 1) U_i/V_m = 32; 2) 2.6; 3) 0.12.

The parameters B (characterizing the stress field) and k [corresponding to the position of the maximum of axial velocity V(y)] are formulas for relative velocity U_i/V_m and are found from the relations

$$k^2 = \int_{\eta}^{1} yf(y,\ B,\ k)\,dy \Big/ \int_{\eta}^{1} (1/y)\,f(y,\ B,\ k)\,dy, \tag{4}$$

$$B = (V_m/U_1)(1-\eta^2) \int_{\eta}^{1} (1/y^3)\,f(y,\ B,\ k)\,dy \Big/ \int_{\eta}^{1} y^2(y-k^2/y)\,f(y,\ B,\ k)\,dy. \tag{5}$$

Figure 2 shows profiles of velocity and viscosity for the values n = 0.64 and η = 0.66, corresponding to the lowest values of these parameters in our experiments. For a relative gap size $\eta \approx 1$, the velocity distribution can be expressed by approximate formulas (Cartesian coordinates, Fig. 1):

$$V(x)/V_m = \int_{-1/2}^{x} x\,(S^2x^2+1)^p\,dx' \Big/ \int_{-1/2}^{1/2} x^2(S^2x^2+1)^p\,dx, \tag{6}$$

$$U(x)/U_i = 1 - \int_{-1/2}^{x} (S^2x'^2+1)^p\,dx' \Big/ \int_{-1/2}^{1/2} (S^2x^2+1)^p\,dx. \tag{7}$$

The parameter S can be calculated as a function of U_i/V_m on the basis of the relation

$$S = \frac{V_m}{U_i} \int_{-1/2}^{1/2} (S^2x^2+1)^p\,dx \Big/ \int_{-1/2}^{1/2} x^2(S^2x^2+1)^p\,dx. \tag{8}$$

2. Stability of a Spiral Flow of Pseudoplastic Fluids

To evaluate the effect of pseudoplasticity on the stability limit, we will resort to a theoretical analysis in which we assume that the secondary flow for a very narrow annular slit is toroidal. The solution of the problem even in this simplified formulation will make it possible to determine dimensionless parameters that describe the stability limit. In accordance with the theory, axisymmetric perturbations of the main flow can be represented in the form

$$V_k' = \hat{V}_k(r)\exp(iat + ibz). \tag{9}$$

To linearize the equations of motion, we make use of perturbations of viscosity

$$\mu = \mu_0 + \mu', \tag{10}$$

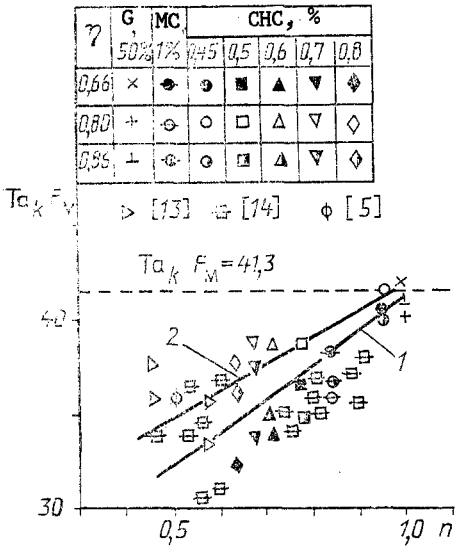

Fig. 3. Stability of a Couette flow of pseudoplastic fluids: theoretical results; 2) results from [12].

$$\mu_0 = K\left[(\dot{\gamma}_{zr})^2 + (\dot{\gamma}_{\theta r})^2\right]^{\frac{n-1}{2}}. \tag{11}$$

Here, μ_0 is the distribution of viscosity in the main flow. The elements of the strain-rate tensor are determined by differential equations (1), (2) or (6), (7)

$$\mu' = \mu_0 (n-1)(\dot{\gamma}_{zr}\dot{\gamma}'_{zr} + \dot{\gamma}_{\theta r}\dot{\gamma}'_{\theta r})/(\dot{\gamma}_{zr}^2 + \dot{\gamma}_{\theta r}^2), \tag{12}$$

μ' is the perturbation of viscosity corresponding to the secondary flow; $\dot{\gamma}_{ij}$ are elements of the strain-rate tensor corresponding to the velocities of the secondary flow V_i'. The linearized stability equation can be changed into a dimensionless eigenvalue formulation of the problem in which Re and Ta are based on viscosity averaged across the gap:

$$\mu_m = \frac{1}{1-\eta}\int_{\eta}^{1} \mu_0(y)\, dy. \tag{13}$$

As a result, we arrive at the operator

$$L(\alpha\beta\eta\, n\, \mathrm{Re}\, \mathrm{Ta}_k) = 0, \tag{14}$$

where α and β are dimensionless parameters corresponding to a and b. The quantity Ta_k plays the role of the eigenvalue. Calculations were performed for a narrow slit $\eta = 0.9$ with the use of profiles (6) and (7). The lowest positive value of Ta_k was obtained for $\beta = \pi$ (square vortical cells). The ranges of the parameters were as follows: $Re < 200$, $0.25 < n < 0.9$.

The results obtained for $V_m = 0$ (stability of a Couette flow of pseudoplastic fluids) are shown in Fig. 3 in the form of the relation $Ta_k(n)$. It can be seen that reinforcement of pseudoplasticity (a reduction in n) reduces the critical value of the Taylor number. This is in complete agreement with the data in [12], which is also shown in Fig. 3. The results of our calculations for $n = 0.9$ (slight pseudoplasticity) are close to the stability limit for the Newtonian analog [7]. The theoretical predictions obtained give an increase in Ta_k with an increase in Re throughout the investigated range of Re and n (the axial flow has a stabilizing effect on the rotational flow). The stability limit is especially heavily dependent on n within the region of very small Re (Fig. 4). A reduction in n results in a very large reduction in Ta_k. This effect gradually weakens with an increase in Re and disappears at $Re > 30$, with all of the points lying on one curve. The results obtained for pseudoplastic fluids at $Re > 30$ coincide with the stability limit for a Newtonian fluid [7]. The use of the dimensionless criteria Re and Ta on the basis of averaged apparent viscosity is reflected in the resulting general relation $Ta_k = f\,Re$ for determination of the stability limit of a spiral flow of pseudoplastic fluids in the range $Re > 30$.

3. Experimental Method and Unit

The stability limit was found by an indirect method based on measurements of the mass flow from the surface of the internal cylinder. It is well known that the formation of a

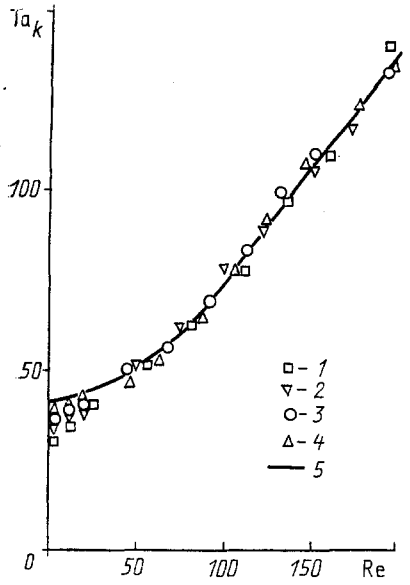

Fig. 4

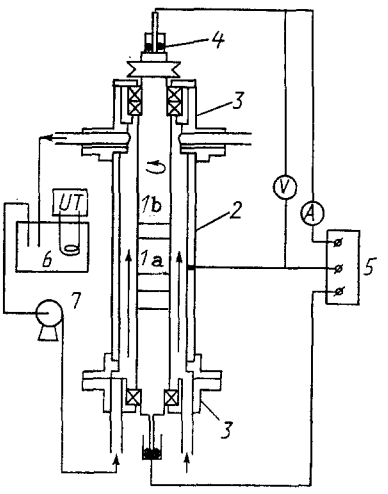

Fig. 5

Fig. 4. Stability of a spiral flow of pseudoplastic fluids: theoretical result for a narrow slit, $\eta = 0.9$: 1) n = 0.25; 2) 0.50; 3) 0.75; 4) 0.90; 5) 1.0 [7].

Fig. 5. Diagram of experimental unit: working section: 1) internal cylinder (a, cathodes; b, anodes); 2) external cylinder; 3) bushings with bearings; 4) mercury current pickoffs; 5) potentiostat; 6) container; 7) pump.

secondary flow is manifest in an appreciable intensification of mass transfer [16]. Measurements with a hot-wire anemometer showed that the most sensitive region is located near the surface of the inside cylinder [17]. This justifies the use of the method we have chosen to calculate the stability limit of a spiral flow.

The mass flows were determined by an electrochemical method [18]. We used solutions of ferricyanides and nickel electrodes. During the occurrence of the polarization-controlled reaction, the following relationship exists between the limiting electric current and the mass transfer coefficient

$$i_{lr} = k_c z_i F_0 c_i. \qquad (15)$$

Thus, the value of the mass-transfer coefficient can be determined from direct measurements of the electrochemical current at the prescribed potential. Figure 5 shows a diagram of the experimental unit we used. It has four main parts: a working section; a container with a thermostat; a circulating pump; an electrical system for electromechanical measurements.

The main component – the working section – is a hollow rotating cylinder which has three sections: an inlet section (200 mm long) made of stainless steel; a cathodic section consisting of four nickel rings insulated from one another (each ring is 18 mm long); an outlet section, serving simultaneously as the anode, in the form of a nickel-plated steel rod. Both ends of this cylinder (the internal cylinder) are placed in bearings which are fastened by stainless steel bushings. The external cylinder, made of Pyrex glass, is placed in the bushings coaxially. We used three replaceable external cylinders with inside radii of 46.4, 50, and 60 mm. The outputs from the cathodes and anode, with a stabilized power supply (potentiostat), were connected to both ends of the inside cylinder through mercury pickoffs.

Working Fluids. We used three types of aqueous solutions: carboxymethylcellulose (CMC) (0.45-0.8 mass %); 1% methylcellulose (MC), glycerin (G) (50%). In accordance with the requirements of the electrochemical method, we added the following to the solutions: 0.2 mole/liter sodium bicarbonate (base electrolyte); 0.01 mole/liter potassium ferrocyanide; 0.005 mole/liter potassium ferricyanide. The solutions exhibited non-Newtonian properties and obeyed an exponential flow law with a flow index between 0.64 and 0.95. The polymer solutions were prepared 24 h before the tests, while the ferri- and ferrocyanides were added

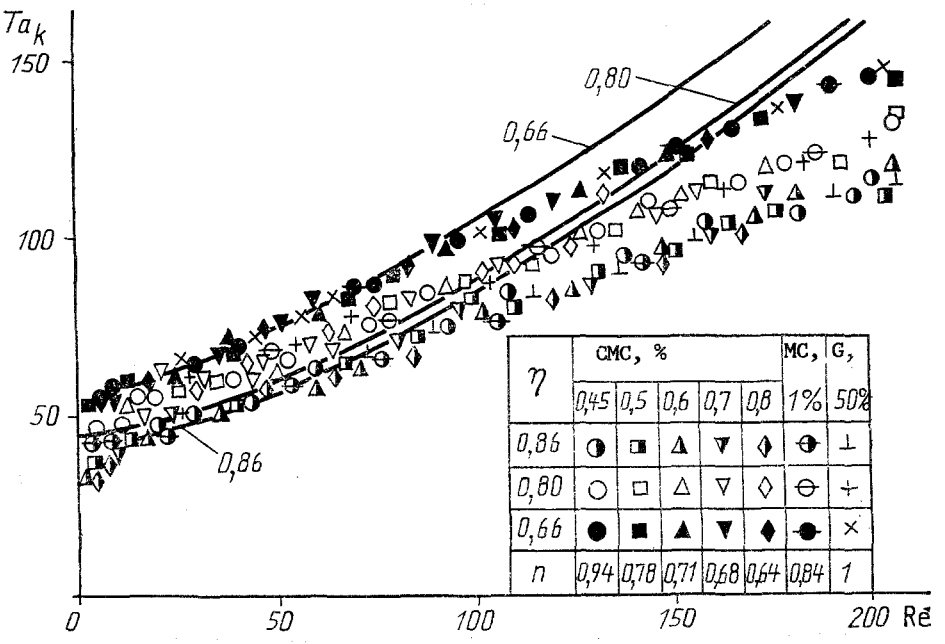

Fig. 6. Stability of the spiral flow of pseudoplastic fluids: points) experimental data; curves) theoretical results for a Newtonian fluid (axisymmetric vortices).

the day of the tests. The entire composition was then injected with gaseous nitrogen. Before the measurements were made, we stabilized the theological properties of the solution by subjecting it to repeated pumping through the channels of the unit.

Measurements of Stability. We determined the dependence of the limiting current i_ℓ on the angular velocity ω_i of the inside cylinder. Measurements were made on a cathode ring positioned 270 mm from the inlet. The speed of rotation was varied while keeping the axial velocity V_m fixed. The current i_ℓ remained nearly constant up to certain speeds, which indicated the absence of secondary flows. A sudden increase in current i_ℓ beginning with a certain value of ω_i was interpreted as the onset of instability. By repeating this procedure for different values of axial velocity V_m, we obtain the required relation $\omega_k = f(V_m)$. The tests were augmented by visual observations for the 0.45% solution of CMC. It was found that the point at which i_ℓ begins to increase corresponds closely to the moment of the appearance of Taylor vortices in the visualization tests.

4. Results

Stability of Couette Flow. The data obtained for very low axial velocities V_m can be used to analyze the stability of Couette flow ($V_m = 0$). This follows from the smallness of the effect of the axial flow on the stability of rotational flow at low Re. Theoretical calculations predict the destabilizing effect of pseudoplasticity on Couette flow. We performed our calculations in the narrow-slit approximation, i.e., with a constant viscosity across the gap. This constancy is not seen for a wide gap, in which case viscosity will be lower near the rotating inside cylinder than near the stationary outside cylinder. The difference in these viscosities will increase with a decrease in the flow index n and the ratio of the radii η. In order to compare data for different n and η, it is necessary to choose the appropriate characteristic viscosity. According to visualization experiments [14], the onset of instability in a pseudoplastic fluid is characterized by toroidal eddies – as in the case of a Newtonian fluid. Making use of the fact that the eddies fill the entire gap, we can take the mean viscosity ($V_m = 0$)

$$\mu_m = \frac{1}{1-\eta}\int_\eta^1 \mu_0(y)\,dy = \\ = K\omega_i^{n-1}(1-\eta)^{\frac{2}{n}-1}\Big/\left(\frac{n}{2}(\eta^{-\frac{2}{n}}-1)\right)^{n-1}\left(\frac{2}{n}-1\right). \tag{16}$$

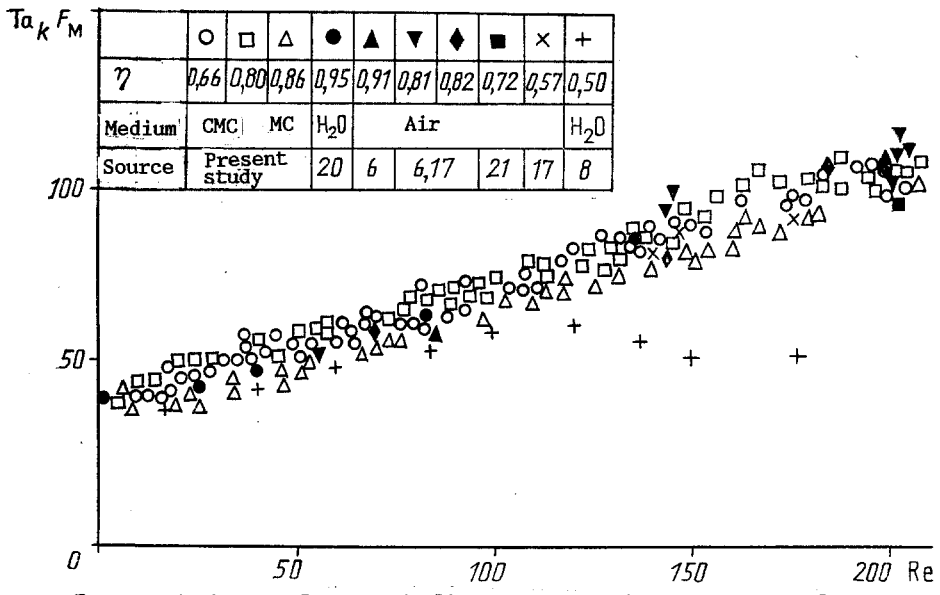

Fig. 7. Stability of spiral flow: general comparison for pseudoplastic and Newtonian fluids.

TABLE 1. Dependence of $Ta_k F_M$ on Re for Different Gap Sizes

Re	η					
	0,86		0,80		0,60	
	Ta_k	$Ta_k F_M$	Ta_k	$Ta_k F_M$	Ta_k	$Ta_k F_M$
0,2	45,6	41,3	48,6	41,8	58,3	39,9
20	46,4	42,0	50,4	43,4	61,6	42,2
60	58,0	52,5	66,5	55,2	75,5	51,7
100	80,4	70,4	88,1	70,8	99,5	68,8
140	110,3	99,9	117,2	100,5	139,8	95,8
200	156,0	141,8	164,4	141,2	177,5	121,6

Measurements made with very low values of axial velocity were analyzed in dimensionless form to determine the Taylor number from the mean viscosity μ_m.

In the comparison, we used the following criterion for the stability of a Couette flow of a Newtonian fluid:

$$Ta_k F_M(\eta) = 41.3,$$
$$F_M(\eta) = \frac{2}{\eta+1}\left(1 - 1.5\,\frac{1-\eta}{1+\eta}\right)^{1/2}. \qquad (17)$$

This criterion was first established by Meksyn [19] and has been shown to be valid for a wide range of η. The results of measurements of the stability of Couette flow (for Re < 3) are shown in Fig. 3 in the form of the dependence of the Taylor number on n. The data from the experiments performed with water–glycerin mixtures is in agreement with the stability criterion for Newtonian fluids. The values of Ta_k for the polymeric fluids turned out to be below the values predicted by this criterion. Reinforcement of pseudoplasticity leads to a reduction in the critical Taylor number. We compared the measurement results with theoretical estimates for the Couette flow of a power-law fluid. It was found that the reduction in Ta_k which occurred in the tests with an intensification of pseudoplasticity was close to the theoretical reduction. These tendencies have been noted by other investigators (see Fig. 3). All of the results were obtained from visualization experiments with aqueous solutions of CMC for η > 0.6. The experimental points lie along the theoretical curve with standard deviations of 12%.

Stability of Spiral Flow. The calculations were based on Eqs. (4) and (5). It was established that $(U_i/V_m) > 2.5$ for all points. An analysis of the velocity profiles led to the conclusion that the distortion of them caused by the axial component has very little

effect on the stability limit. However, it was also found that the viscosity field may become quite nonuniform when axial velocity is high (Fig. 2).

It was established from a simplified theoretical analysis of the stability problem that by using the mean viscosity in the criteria Re and Ta, it is possible to obtain a generalized expression for the stability limit of a spiral flow of pseudoplastic fluids.

The results of tests concerning the stability of the flow of pseudoplastic fluids can be generalized in accordance with the proposed method [Re and Ta_k being based on the mean viscosity μ_m, Eq. (13)]. The results for three gap sizes are shown in Fig. 6. The experimentally obtained stability limits can be divided into two ranges: 1) $Re < 20$; 2) $20 < Re < 200$. In the first range, with low Reynolds numbers, the axial flow typically has little effect on the stability of the rotational motion. Intensification of pseudoplasticity lowers the critical value of the Taylor number (for fixed Re). This tendency is stronger at $Re \to 0$ but nearly disappears at $Re = 20$. The stabilizing effect of the axial flow is more pronounced above this value. The data for polymer solutions is close to the results obtained for Newtonian fluids (water–glycerin mixtures). On the whole, the results confirm the previous conclusions to the effect that the conditions for the onset of instability can be represented through values of Re and Ta based on mean apparent viscosity μ_m.

5. Generalization of the Results

To cast the results obtained here in a more universal form, let us examine the effect of the geometric parameter η on the stability limit. The problem of the stability of a spiral flow of a Newtonian fluid in a wide slit was solved with the assumption of an axisymmetric secondary flow. We regarded the stability equation, taken from [7], as constituting an eigenvalue problem for Ta_k. Here, the number Re is a parameter. Calculations were performed for an initial range $Re < 200$ and several values $0.6 < \eta < 0.9$ (the results are shown in Table 1). It was found that the use of a modified Taylor number $Ta_k F_M$ makes it possible to generalize theoretical results for individual values of η. This is also evident from Table 1. We made use of this finding in our analysis of the experimental results. For a generalized comparison of results obtained with different $\eta = (R_1/R_2)$, we transformed the test data into the dependence of the modified Taylor number $Ta_k F_M$ on Re (Fig. 7). All of the experimental points lie along one curve (to within 10%). Thus, we determined a generalized stability limit for spiral flows of pseudoplastic fluids which is valid for the conditions $\eta > 0.6$ and $Re < 200$.

The agreement with measurements made by other investigators for Newtonian fluids (water and air) in this range of Re turned out to be good. The generalized stability limit is valid at low Re, where the rotational flow undergoes monotonic stabilization by the axial flow. This situation is disturbed at $\eta = 0.5$ [8].

CONCLUSIONS

The results of measurement of stability were correlated with the use of Reynolds and Taylor numbers based on mean viscosity. The stability limit for Couette flow can be expressed through the functional dependence of the modified critical Taylor number $Ta_k F_M$ on the flow index n. This dependence, characteristic of all "power-law" pseudoplastic fluids, is close to the theoretical predictions and expresses the destabilizing effect of pseudoplasticity on rotational motion.

Beyond the initial range $Re > 20$, pseudoplasticity has almost no effect on the stability of spiral flow. In the range where the axial flow monotonically stabilizes the spiral flow, stability is described by the generalized dependence of the modified Taylor number $Ta_k F_M$ on the Reynolds number. This dependence is valid for all pseudoplastic fluids (including Newtonian fluids) and relative gap sizes $\eta = R_1/R_2$.

NOTATION

a, frequency, sec^{-1}; b, wave number [Eq. (9)], sec^{-1}; $B = \pi R_2^3 \Delta p/(M_0 L)$, parameter; C_ℓ, concentration of reacted ions, $kmoles/m^3$; $d = R_2 - R_1$, width of slit, m; $f(\cdot\cdot)$, function determined by Eq. (3); F_0, Faraday constant, sec/kmole; F_M, Meksyn geometric parameter; i_ℓ, limiting current, A/m^2; K, consistency index, $N \cdot sec/m^2$; $k = r_m/R_2$, parameter; k_c, mass-transfer coefficient, m/sec; M_0, turning moment per unit length, N; n, flow index; $p = 1/2n - 1/2$, parameter; $\Delta P/L$, pressure loss per unit length of the annular channel, N/m^3; r, radial coordi-

nate, m; r_m, radial position of velocity-profile maximum, m; R_1, R_2, internal and external radii of slit, m; $Re = V_m \rho 2d/\mu_m$, Reynolds number; $S = (\Delta P/L)2\pi R_2^2 d/M_0$, parameter; $Ta = \omega_i d^{3/2} R_1^{1/2} \rho/\mu_m$, Taylor number; U, tangential velocity, m/sec; U_i, tangential velocity on the surface of the internal cylinder, m/sec; V, axial velocity, m/sec; V_m, mean axial velocity, m/sec; V_k', component of perturbation velocity, m/sec; V_k, amplitude; $\hat{V}_k$, perturbation, m/sec; $x = (r - (R_1 + R_2)/2)d$, dimensionless radial coordinate; $y = r/R$, radial corodinate; Z_i, number of electrons participating in the electrochemical reaction; μ, apparent viscosity, Pa·sec; μ_0, apparent viscosity of the main flow, Pa·sec; μ', perturbation of the field of apparent viscosity, Pa·sec; μ_m, mean value of apparent viscosity, Pa·sec; $\dot{\gamma}_{ij}$, components of the strain-rate tensor for the main flow, sec^{-1}; $\dot{\gamma}_{ij}'$, components of the strain-rate tensor for the perturbed flow, sec^{-1}; ω, angular velocity, rad/sec; ω_i, angular velocity of the internal cylinder, rad/sec.

LITERATURE CITED

1. I. Kaye and E. C. Elgar, Trans. ASME, 80, 753-795 (1958).
2. W. Tobler, Filtr. Sep., 19, 329-332 (1982).
3. R. L. Mullen, A. Prekwas, M. J. Braun, and R. C. Hendrichs, Heat Transfer and Fluid Flow in Rotating Machinery, Hemisphere, Washington (1987).
4. D. R. Gabe and F. C. Walsh, J. Appl. Electrochem., 13, 3-22 (1983).
5. C. Nouar, R. Davienne, and Lebouche, Int. J. Heat Mass Transfer, 39, 639-647 (1987).
6. P. L. Greaves, R. I. Groswenor, and B. W. Martin, Int. J. Heat Fluid Flow, 4, 187-197 (1983).
7. R. C. Di Prima and A. Pridor, Proc. R. Soc., London, Ser. A, 366, 555-573 (1979).
8. D. I. Takeuchi and D. F. Jankowski, J. Fluid Mech., 28, 255-263 (1988).
9. W. M. Jones, J. Non-Newtonian Fluid Mech., 28, 255-263 (1988).
10. Z.-S. Sun and M. M. Denn, AIChE J., 18, 1010-1015 (1972).
11. R. F. Ginn and M. M. Denn, AIChE J., 15, 450-454 (1969).
12. V. S. Belokon', Inzh.-Fiz. Zh., 24, No. 4, 719-724 (1973).
13. V. Sinevic, R. Kuboi, and A. W. Nienow, Chem. Eng. Sci., 41, 2915 (1986).
14. Z. Kemblobski and J. Duda, Zesz. Nauk Politech. Lodz., 7, 129-135 (1977).
15. S. Wronski, M. Jastrzebski, and L. Rudniak, Inz. Chem. Proc., 6, No. 4 (1989).
16. K. Kataoka, H. Doi, and T. Komai, Int. J. Heat Mass Transfer, 20, 57-63 (1977).
17. N. Gravas and B. W. Martin, J. Fluid Mech., 86, 385-394 (1978).
18. F. P. Berger and A. Ziai, Chem. Eng. Res. Dev., 61, 377-382 (1983).
19. D. Meksyn, New Methods in Laminar Boundary Layer Theory, London (1961).
20. H. A. Snyder, Proc. R. Soc. London, Ser. A, 295, 198-214 (1962).
21. K. N. Astill, J. Heat Transfer, Trans. ASME, 86, 383-391 (1964).